US of the Pediatric Female Pelvis: A Clinical Perspective[1]

Laurent Garel, MD • Josée Dubois, MD • Andrée Grignon, MD
Denis Filiatrault, MD • Guy Van Vliet, MD

ONLINE-ONLY CME

See www.rsna.org/education/rg_cme.html.

LEARNING OBJECTIVES

After reading this article and taking the test, the reader will be able to:

- Describe the morphologic changes in the genital organs induced by puberty in females.
- Discuss the contribution of US in a variety of conditions in childhood, especially assessment of hormonal status and investigation of pelvic pain or pelvic masses.
- Describe the basic features of the embryology of the genital tract in females and of sexual differentiation in the fetus.

When investigating pelvic pathologic conditions in female pediatric patients, one needs to be aware of the developmental changes that take place around puberty. The prepubertal uterus is thin, with a fundus equal in size to the cervix. Owing to the hormonal stimulation of puberty, the uterus enlarges and the fundus becomes prominent. The ovaries are demonstrated with ultrasonography (US) at all ages. Ovarian volume increases after 6 years of age. Microcystic follicles are normally seen throughout childhood. US is the modality of choice for imaging the pediatric female pelvis. The main indications for pelvic US in the pediatric age group are pubertal precocity or pubertal delay, pelvic pain or pelvic masses, and ambiguous genitalia. Vaginal bleeding in the prepubertal child can be due to a vaginal foreign body, vaginal rhabdomyosarcoma, or precocious puberty. Common causes of primary amenorrhea in teenagers include gonadal dysgenesis (Turner syndrome) and müllerian (uterovaginal) anomalies. Pelvic pain or pelvic masses in pediatric patients can be due to ovarian torsion, hemorrhagic ovarian cyst, pelvic inflammatory disease, or ectopic pregnancy.

Index terms: Children, genitourinary system, 85.1298 • Genitourinary system, abnormalities, 85.147 • Menstruation, 85.147 • Ovary, torsion, 852.899 • Pelvic organs, abnormalities, 85.147 • Pelvic organs, neoplasms, 85.30 • Ultrasound (US), in infants and children, 85.1298

RadioGraphics 2001; 21:1393–1407

[1]From the Departments of Medical Imaging (L.G., J.D., A.G., D.F.) and Endocrinology (G.V.V.), Sainte-Justine Hospital, 3175 Côte Sainte-Catherine, Montreal, Quebec, Canada H3T 1C5; and the Departments of Radiology (L.G., J.D., A.G., D.F.) and Endocrinology (G.V.V.), University of Montreal. Presented as an education exhibit at the 2000 RSNA scientific assembly. Received March 28, 2001; revision requested April 26 and received May 28; accepted May 29. **Address correspondence to** L.G. (e-mail: *laurent_garel@ssss.gouv.qc.ca*).

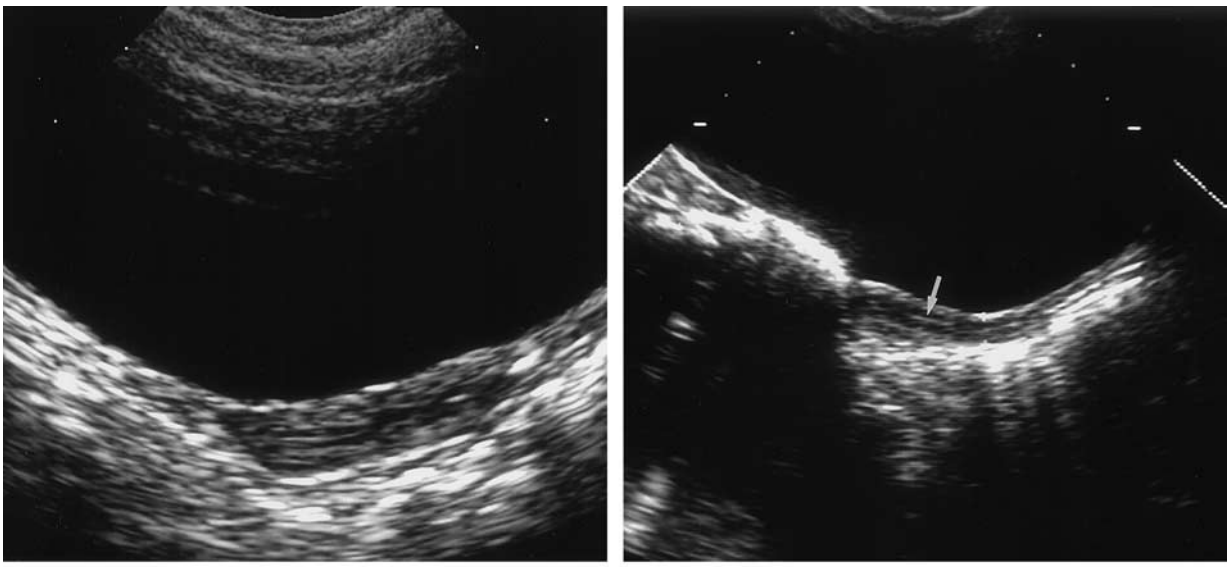

a. b.

Figure 2. Prepubertal uterus. **(a)** Longitudinal US scan obtained in a 5-year-old girl shows a tubular uterus; the anteroposterior diameter is 6 mm. **(b)** Longitudinal US scan obtained in a 6-year-old girl shows the endometrial lining as a thin echogenic line (arrow).

Introduction

Ultrasonography (US) remains the most useful modality for imaging pediatric genital organs.

Knowledge of the simple embryology of the genital tract and basic physiologic features of puberty is necessary in investigating cases of precocious puberty, amenorrhea, pelvic pain, pelvic masses, or ambiguous genitalia in children.

This article reviews the following topics from a clinically oriented perspective: (*a*) the normal US anatomy of genital organs in infants and children, (*b*) US assessment of the hormonal status of pediatric females, (*c*) US investigation of prepubertal bleeding, (*d*) work-up of primary amenorrhea in teenagers, (*e*) the diagnostic value of US in pediatric patients with pelvic pain or pelvic masses, and (*f*) the contribution of US in patients with ambiguous genitalia.

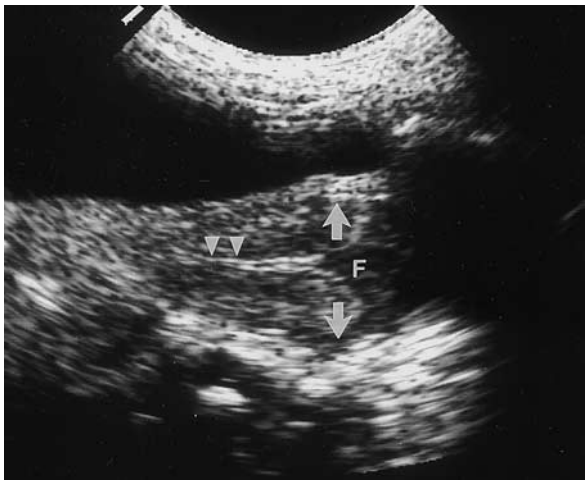

Figure 1. Neonatal uterus. Longitudinal US scan shows a prominent cervix (arrows) and a visible endometrium (arrowheads). Some fluid (*F*) is seen within the vagina.

Normal US Anatomy of Genital Organs in Infants and Children

The Uterus

Uterine anatomy changes during pediatric life (1).

The neonatal uterus is prominent (Fig 1) under the influence of maternal and placental hormones (2,3). The cervix is larger than the fundus (fundus-to-cervix ratio = 1/2), the uterine length is approximately 3.5 cm, and the maximum thickness is approximately 1.4 cm; the endometrial lining is often echogenic. Some fluid can also be seen within the endometrial cavity.

The prepubertal uterus has a tubular configuration (Fig 2a) (anteroposterior cervix equal to anteroposterior fundus) or sometimes a spade shape (anteroposterior cervix larger than anteroposterior fundus) (4–8). The endometrium is normally not apparent; however, high-frequency transducers can demonstrate the central lining in some cases (Fig 2b). The length is 2.5–4 cm; the thickness does not exceed 10 mm.

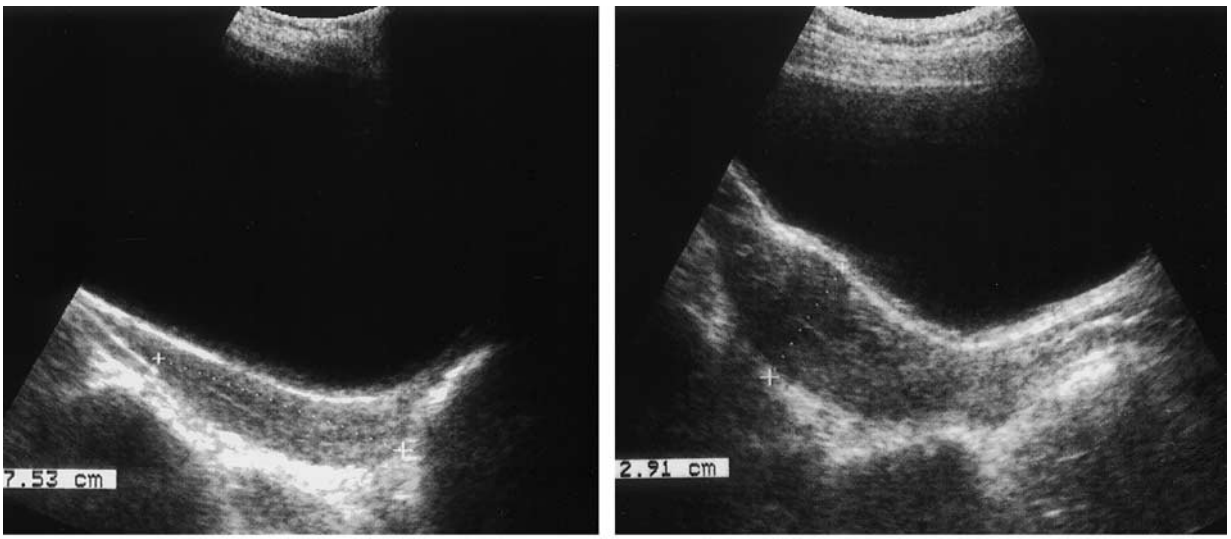

a. b.

Figure 4. Effect of overfilling of the bladder on uterine shape in a 12-year-old girl. **(a)** Longitudinal US scan shows an overfilled bladder compressing the uterus, making the fundal prominence less apparent than in **b**. **(b)** Longitudinal US scan obtained after partial emptying of the bladder clearly shows that the fundus is thicker than the cervix.

Figure 3. Postpubertal uterus in a 13-year-old girl. Longitudinal US scan shows that the fundus is larger than the cervix; the endometrium is well seen.

Pediatric Ovarian Volumes

Age (y)	Mean Volume (cm^3)	Standard Deviation
1	1.05	0.7
2	0.67	0.35
3	0.7	0.2
4	0.8	0.4
5	0.9	0.02
6	1.2	0.4
7	1.3	0.6
8	1.1	0.5
9	2.0	0.8
10	2.2	0.7
11	2.5	1.3
12	3.8	1.4
13	4.2	2.3

Sources.—References 9 and 10.

The pubertal uterus has the adult pear configuration (fundus larger than cervix) (fundus-to-cervix ratio = 2/1 to 3/1) (4–8) (Fig 3) and is 5–8 cm long, 3 cm wide, and 1.5 cm thick. The endometrial lining is seen and varies with the phases of the menstrual cycle. Overfilling of the bladder can modify the uterine shape (Fig 4).

The Ovaries

Ovarian size is usually described by assessment of the ovarian volume: $V = ½$ length × width × depth (simplified formula for a prolate ellipse).

In infants, measurements are greater than previously reported, with an average of slightly greater than 1 cm^3 for the first year of life and 0.67 cm^3 for the second year (9,10). The mean ovarian volume in girls less than 6 years of age is less than or equal to 1 cm^3. The increase in ovarian volume begins after 6 years of age (Table). In prepubertal girls (6–10 years old), ovarian volumes range from 1.2 to 2.3 cm^3. In premenarchal girls (11–12 years old), ovarian volumes range from 2 to 4 cm^3. In postmenarchal girls, the ovarian volume averages 8 cm^3 (range, 2.5–20 cm^3).

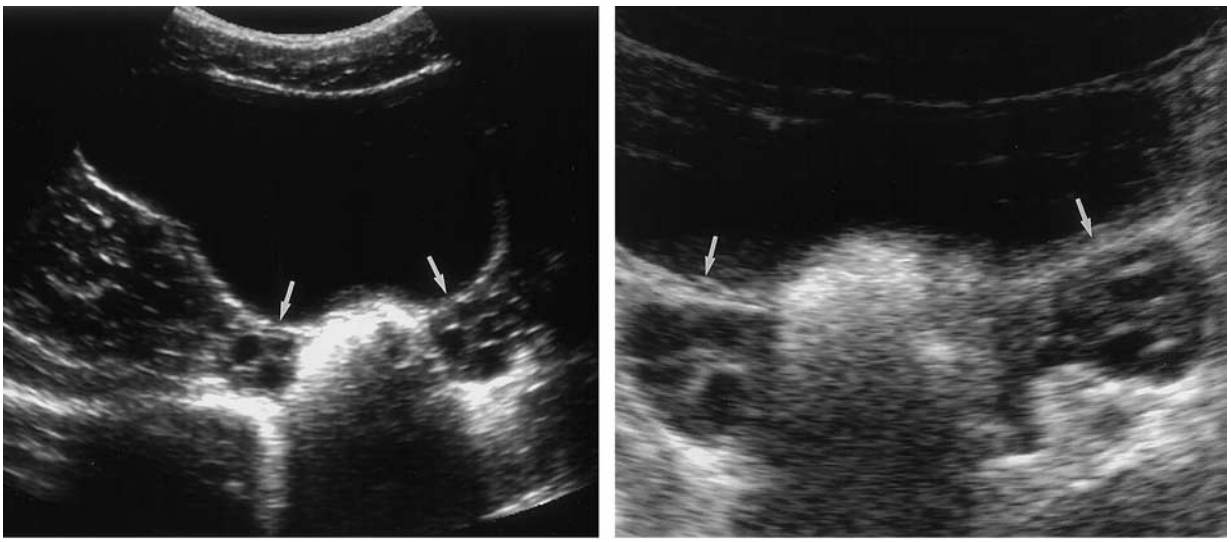

a. b.

Figure 5. Microcystic follicles. **(a)** Transverse US scan obtained in a 1-month-old girl shows normal ovaries (arrows) with visible follicles. The ovarian volume is 1 cm^3. **(b)** Transverse US scan obtained in a 6-year-old girl shows normal ovaries (arrows) with visible follicles. The ovarian volume is 2 cm^3.

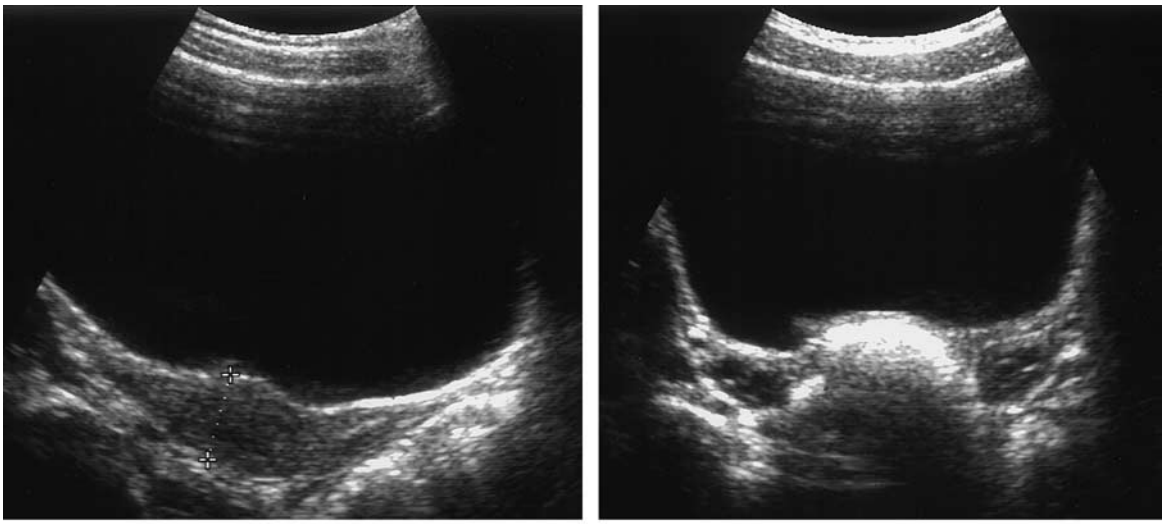

a. b.

Figure 6. US assessment of hormonal status in an 8-year-old girl (bone age = 11 years). **(a)** Longitudinal US scan shows that the uterus has a postpubertal shape. The fundus is 1.75 cm in anteroposterior diameter. **(b)** Transverse US scan shows that the ovaries are not indicative of the postpubertal status, since they have a similar appearance with visible follicles at all ages. The difference is mainly in the size of the ovary.

Normal microcystic follicles are routinely imaged (in 84% of cases from birth to 24 months of age and in 68% of cases between 2 and 12 years of age) (Fig 5) (11).

Confusing discrepancies are found in the literature regarding cutoff values for ovarian volume (vs age, vs pubertal stage, right vs left) (4–8) and regarding the terminology for ovarian echostructure (solid, microcystic, paucicystic, multicystic, macrocystic, major isolated cyst) (6). From a practical standpoint, the following measurements can be considered as upper values for prepubertal girls: Uterine length = 4.5 cm, uterine thickness = 1 cm (the single most useful criterion), and ovarian volume = 4–5 cm^3.

US Assessment of Hormonal Status of Pediatric Females

Definitions

The term *thelarche* refers to the onset and progress of breast development. The term *adrenarche* refers to the onset and progress of pubic and axillary hair development. The term *menarche* refers to the first episode of vaginal bleeding originating

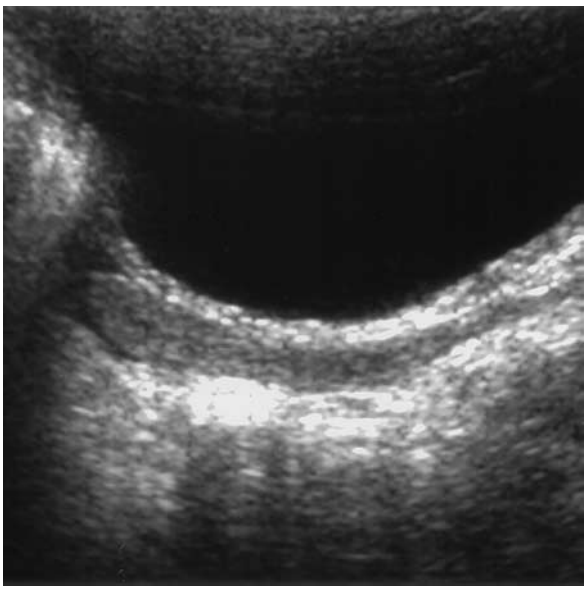

Figure 7. Premature thelarche in an 8-year-old girl (bone age = 8 years). Longitudinal US scan shows a prepubertal uterus (anteroposterior thickness = 5 mm).

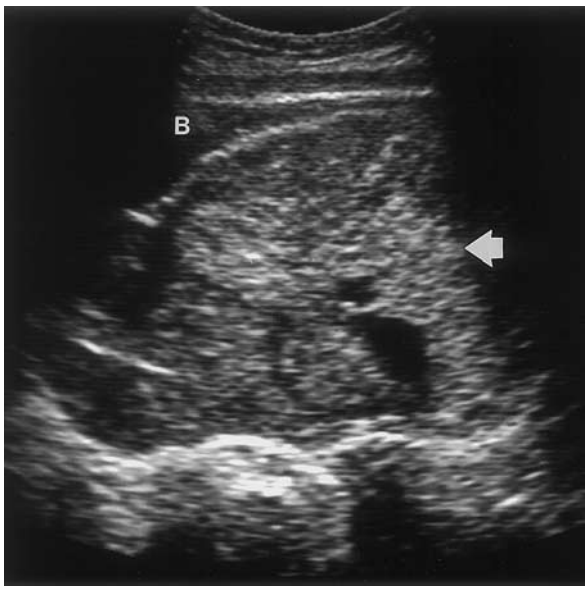

Figure 8. Rhabdomyosarcoma in an 18-month-old girl with vaginal bleeding. Longitudinal US scan of the pelvis clearly shows a large, solid mass within the vagina (arrow). *B* = bladder.

from the uterus (which occurs at a mean of 12.7 years in the United States).

The onset of pubarche is initiated by the adrenal gland (androstenedione-estrone), but the completion of thelarche and menarche requires a more potent hormone (estradiol) from the ovary.

Pelvic Features of Estrogen Stimulation

At US, estrogen stimulation is indicated by increased thickness and volume of the uterus; swelling of the fundus (Fig 6a) (fundus larger than cervix, fundocervical ratio > 2); and the presence of an echogenic endometrium.

The appearance of the ovaries is less useful because of the overlapping of measurements in the literature and because of the normal visibility of follicles at all ages (Fig 6b) (5,11).

Isolated Premature Adrenarche and Isolated Premature Thelarche

No significant differences in pelvic US parameters (fundocervical ratio, uterine length and thickness, ovarian volume) are found between patients with isolated premature adrenarche or isolated premature thelarche and age-matched control patients (Fig 7) (6,12).

US Investigation of Prepubertal Bleeding

Vaginal bleeding in the prepubertal child can be due to a vaginal foreign body, vaginal rhabdomyosarcoma, or precocious puberty. Hemangiomas and vascular malformations are also causes of prepubertal vaginal bleeding.

Vaginal Foreign Body

Vaginal foreign bodies are seen in 18% of children with vaginal bleeding and discharge and in 50% of children with vaginal bleeding and no discharge. A retained vaginal foreign body can be demonstrated at US as a slight indentation of the posterior bladder wall (13); acoustic shadowing is characteristic but not always present.

Vaginal Rhabdomyosarcoma

Vaginal rhabdomyosarcomas are commonly botryoid and are almost exclusively found in very young children. At US, a vaginal rhabdomyosarcoma appears as a large, solid, heterogeneous or hypoechoic mass posterior to the bladder (Fig 8). According to recent publications by the International Society of Pediatric Oncology (14) and the Intergroup Rhabdomyosarcoma Study Group (15), the overall survival rate in nonmetastatic rhabdomyosarcoma of the genital tract is 91% at 5 years.

Precocious Puberty

Precocious puberty is defined as complete sexual development (including menarche) before 8 years of age. Precocious puberty is classified into two types: central and peripheral.

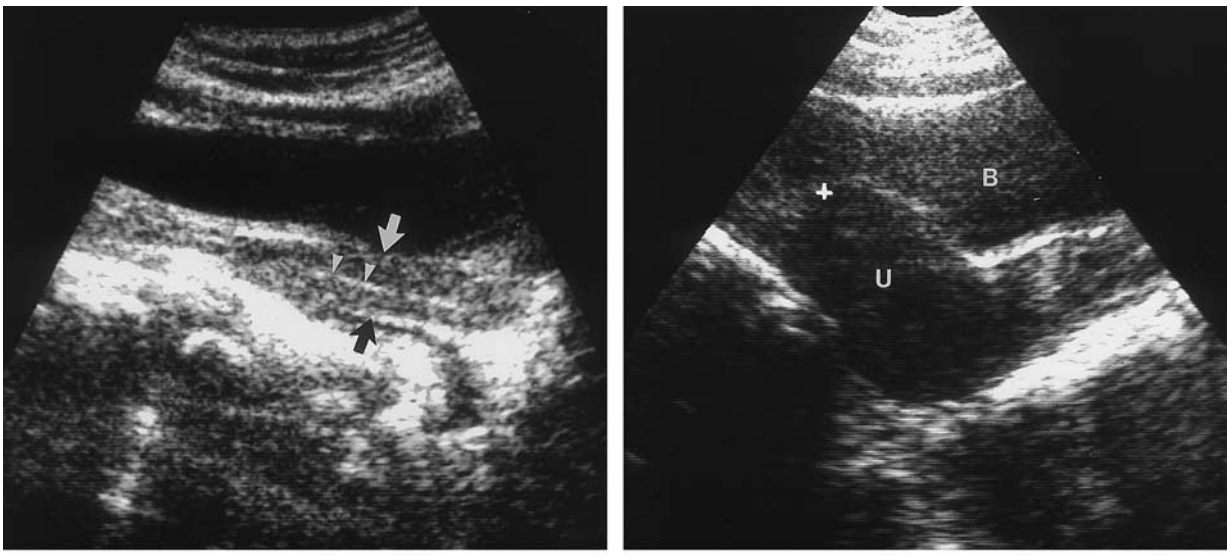

a. b.

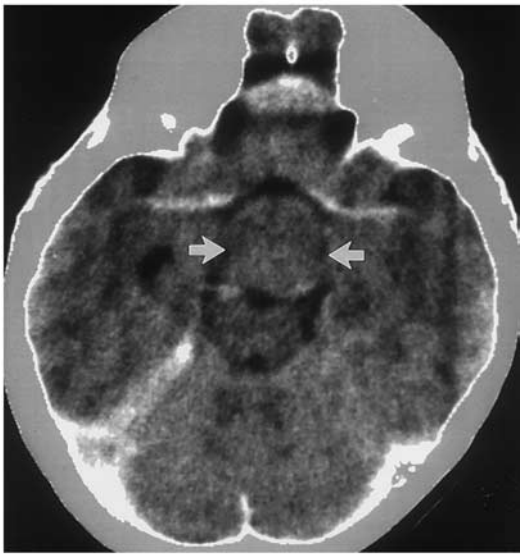

c.

Figure 9. Central precocious puberty in a 5½-year-old girl. **(a)** Longitudinal US scan obtained for assessment of urinary tract infection at 7 months of age shows a prepubertal uterus (arrows). Note the visible endometrium (arrowheads). **(b)** Longitudinal US scan of the uterus (*U*) obtained at 5½ years of age shows the features of estrogen stimulation. *B* = bladder. **(c)** Contrast material–enhanced computed tomographic (CT) scan shows a hamartoma of the tuber cinereum (arrows).

Central precocious puberty (true precocious puberty) is gonadotropin-dependent. This entity is idiopathic in approximately two-thirds of cases. Central nervous system conditions leading to central precocious puberty are space-occupying lesions such as tuber cinereum hamartoma (Fig 9) or increased intracranial pressure (eg, postmeningitis hydrocephalus). The augmentation of uterine and ovarian volumes shown at US occurs prior to the typical changes in secretion patterns of luteinizing hormone and follicle-stimulating hormone revealed with the luteinizing hormone–releasing hormone test (12). If follow-up US is performed during treatment with long-acting gonadotropin-releasing hormone analogues, the scans show decreased volume of the uterus and ovaries and a hormonal status appropriate for age (16,17).

Peripheral precocious puberty (precocious pseudopuberty) is gonadotropin-independent. McCune-Albright syndrome consists of the association of café-au-lait spots, fibrous dysplasia, and peripheral sexual precocity.

Autonomous ovarian follicular cysts are the most frequent cause of peripheral precocious puberty. Bone age is often normal. Serum assays show a high estradiol level, low levels of follicle-stimulating hormone and luteinizing hormone, and no response to stimulation with luteinizing hormone–releasing hormone (18,19).

US demonstrates a stimulated uterus and a unilateral follicular ovarian cyst (19,20), which is characterized by the daughter cyst sign (Fig 10) (21). Spontaneous regression of the symptoms at clinical examination and the ovarian cyst at US alternates with variable recurrences (19); conservative management is the favored option in most cases. Evidence of McCune-Albright syndrome can develop later (19).

Autonomous ovarian follicular cysts are far more common than estrogen-secreting neoplasms such as granulosa cell tumors or gonadoblastomas.

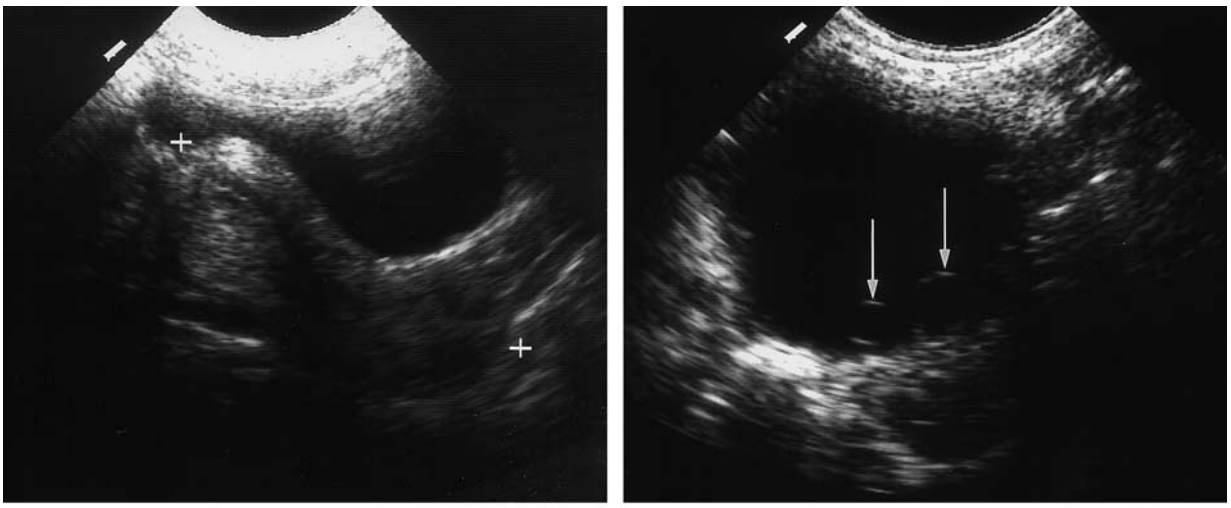

a. b.

Figure 10. Peripheral precocious puberty in an 11-month-old girl. **(a)** Longitudinal US scan shows an obviously stimulated uterus (between cursors). **(b)** Transverse US scan of the cystic left ovary shows two follicles (arrows) within the main cyst (the daughter cyst sign).

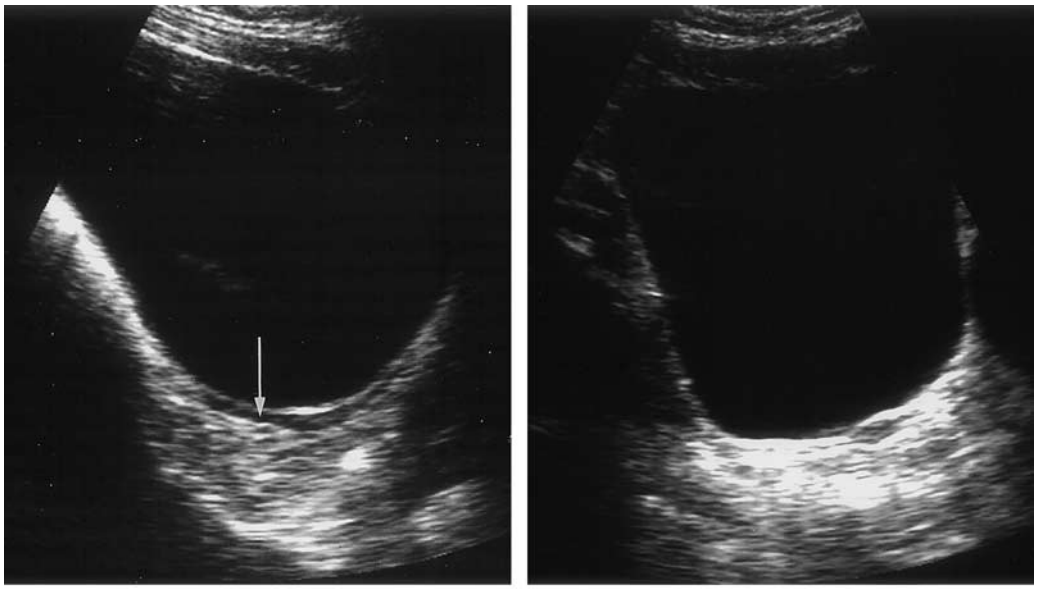

a. b.

Figure 11. Turner syndrome in a 12-year-old girl. **(a)** Longitudinal US scan shows a minute uterus (arrow). **(b)** Transverse US scan shows no visible ovarian tissue.

Work-up of Primary Amenorrhea in Teenagers

Primary amenorrhea is defined as (*a*) no menarche by 16 years of age, (*b*) no thelarche nor adrenarche by 14 years of age, or (*c*) no menarche more than 3 years after adrenarche and thelarche.

The presence or absence of secondary sexual development at clinical examination and müllerian structures at US is the basis for selective ordering of laboratory tests. Common causes include gonadal dysgenesis (Turner syndrome) (33% of cases), müllerian (uterovaginal) anomalies (20%), hypothalamic-pituitary causes (15%), constitutional delay (often familial) (10%), and other causes (eg, systemic, psychiatric) (22%).

Turner Syndrome

Patients with XO karyotype (approximately 70% of those with Turner syndrome) have a prepubertal uterus and nonvisualized or streaky ovaries (Fig 11) (22,23). In rare instances, especially in mosaic karyotypes, the ovaries can be normal in appearance (24). Spontaneous puberty occurs in 5%–15% of patients with Turner syndrome (25).

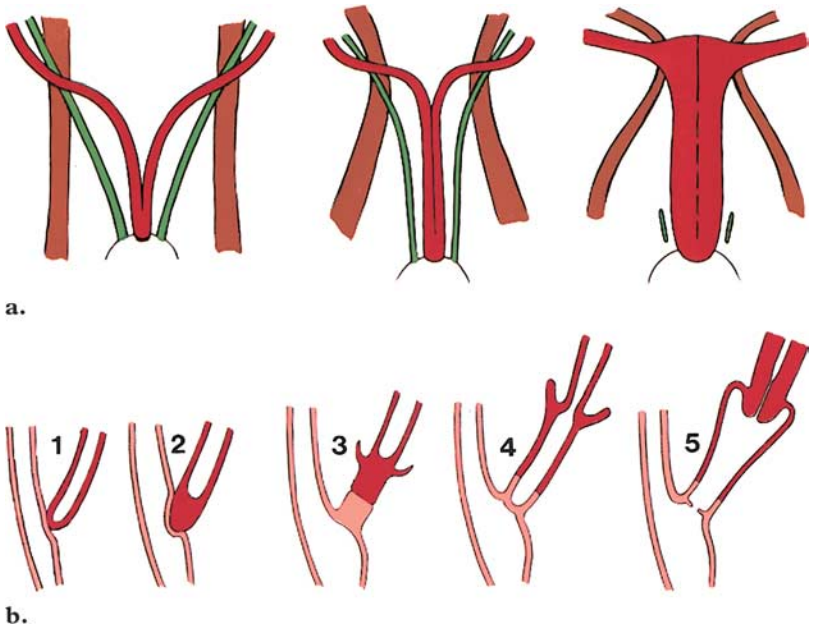

Figure 12. Embryologic development of the uterus and vagina. **(a)** Diagrams show that both müllerian ducts (red area) fuse on the midline to form the uterus. The proximal part of the duct gives rise to the fallopian tube. The wolffian ducts (green areas) regress. The distal remnant of the wolffian duct forms the Gartner duct. **(b)** Diagrams show that the uterovaginal canal (red area) reaches the urogenital sinus (pink area) (*1*). The vaginal plate develops (*2*), proliferates (*3*), and undergoes canalization (*4*). The vagina is formed by both the müllerian ducts and the urogenital sinus (*5*).

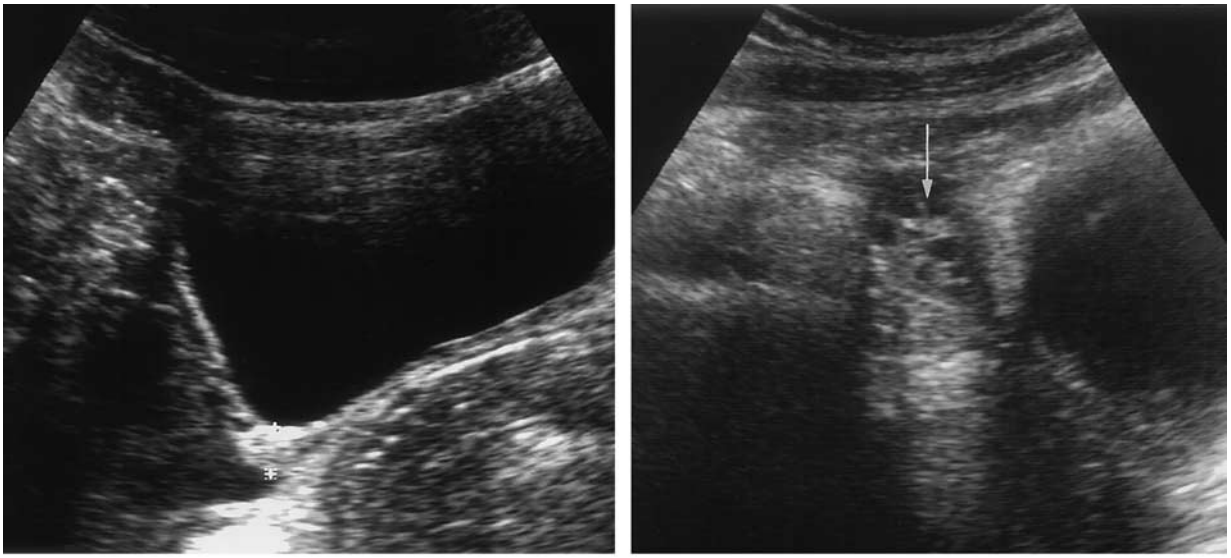

Figure 13. Müllerian agenesis in a 17-year-old girl with primary amenorrhea and normal secondary sexual features. **(a)** Longitudinal US scan of the pelvis shows a rudimentary uterus (between cursors). **(b)** Longitudinal US scan shows a normal right ovary (arrow). The left ovary was also normal.

Müllerian Anomalies

The classification of müllerian anomalies is based on embryologic steps of lateral and vertical fusion.

During lateral fusion, the müllerian ducts develop at 5–6 weeks gestational age from the coelomic epithelium in conjunction with and lateral to the wolffian (mesonephric) ducts. They fuse at about 7–9 weeks gestational age on the midline to form the uterovaginal canal (Fig 12a).

During vertical fusion at 8 weeks gestational age, the uterovaginal canal reaches the urogenital sinus at the müllerian tubercle; the urogenital sinus results from separation of the cloaca into the urogenital sinus and rectum. At the same time, the vaginal plate develops distally. It proliferates first and then undergoes canalization (Fig 12b). Therefore, the vagina is formed by both the müllerian ducts (upper two-thirds or upper four-fifths, depending on the author) and the urogenital sinus (lower one-third or lower one-fifth) (26).

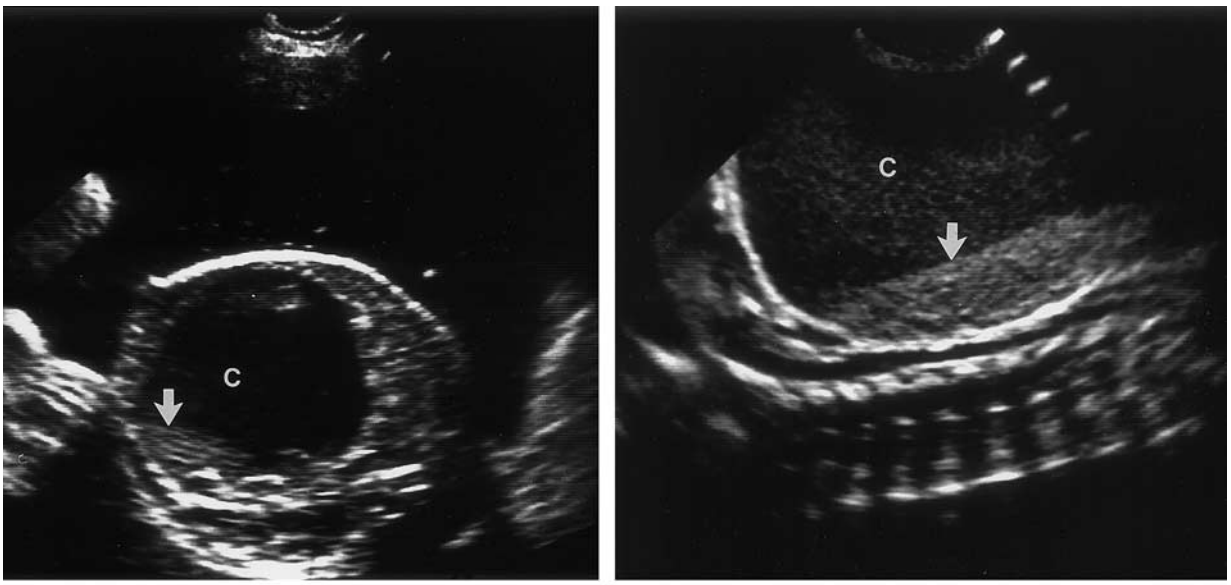

a. b.

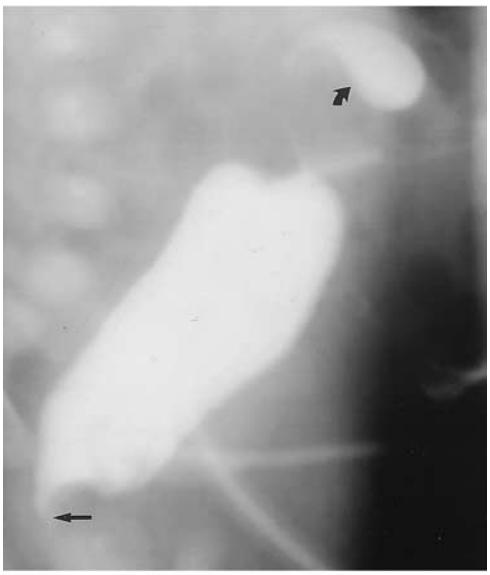

c.

Figure 14. Neonatal hematometrocolpos. **(a)** Transverse US scan of a third-trimester fetus shows a huge cystic mass (*C*) with a fluid-debris level (arrow). The mass fills almost the entire abdomen. **(b)** Longitudinal US scan obtained in the same patient as a newborn shows the mass (*C*), which still has a fluid-debris level (arrow). **(c)** Radiograph obtained with contrast material administered through the draining catheter shows evidence of distal vaginal atresia (straight arrow) and reflux of contrast material within the uterine cavity (curved arrow).

Müllerian anomalies are classified into (*a*) müllerian agenesis, (*b*) disorders of lateral fusion (duplication defects) with or without obstruction, and (*c*) disorders of vertical fusion (canalization defects) with or without obstruction. Because of the frequent association between anomalies of lateral fusion and anomalies of vertical fusion, it is practical to consider these anomalies according to the presence or absence of obstruction.

Müllerian Agenesis.—Müllerian agenesis (Mayer-Rokitansky-Küster-Hauser syndrome) is the second most common cause of primary infertility after gonadal dysgenesis (27,28). Müllerian agenesis is characterized by vaginal atresia associated with an absent or rudimentary uterus (unicornuate or bicornuate) and normal ovaries (Fig 13). The karyotype is normal (46,XX). Renal anomalies (agenesis, ectopia) occur in 50% of cases; skeletal or spinal anomalies occur in 12% of cases. In 6%–10% of patients, functioning endometrium may be present within the rudimentary uterus, resulting in unilateral hematometra.

Obstructive Müllerian Anomalies.—Most cases of hydrometrocolpos in the neonate are associated with a urogenital sinus or cloacal malformation (29,30). Congenital uterovaginal obstructions appear on third-trimester US scans as a pelviabdominal cystic mass with a fluid-debris level (Fig 14). The kidneys are often obstructed and dysplastic. Teenagers with obstructive uterovaginal anomalies present with amenorrhea and cyclic abdominal pain; US is very valuable in differentiating the frequent case of hemato(metro)colpos due to imperforate hymen (Fig 15) or transverse vaginal septum from the rare case of hematometra

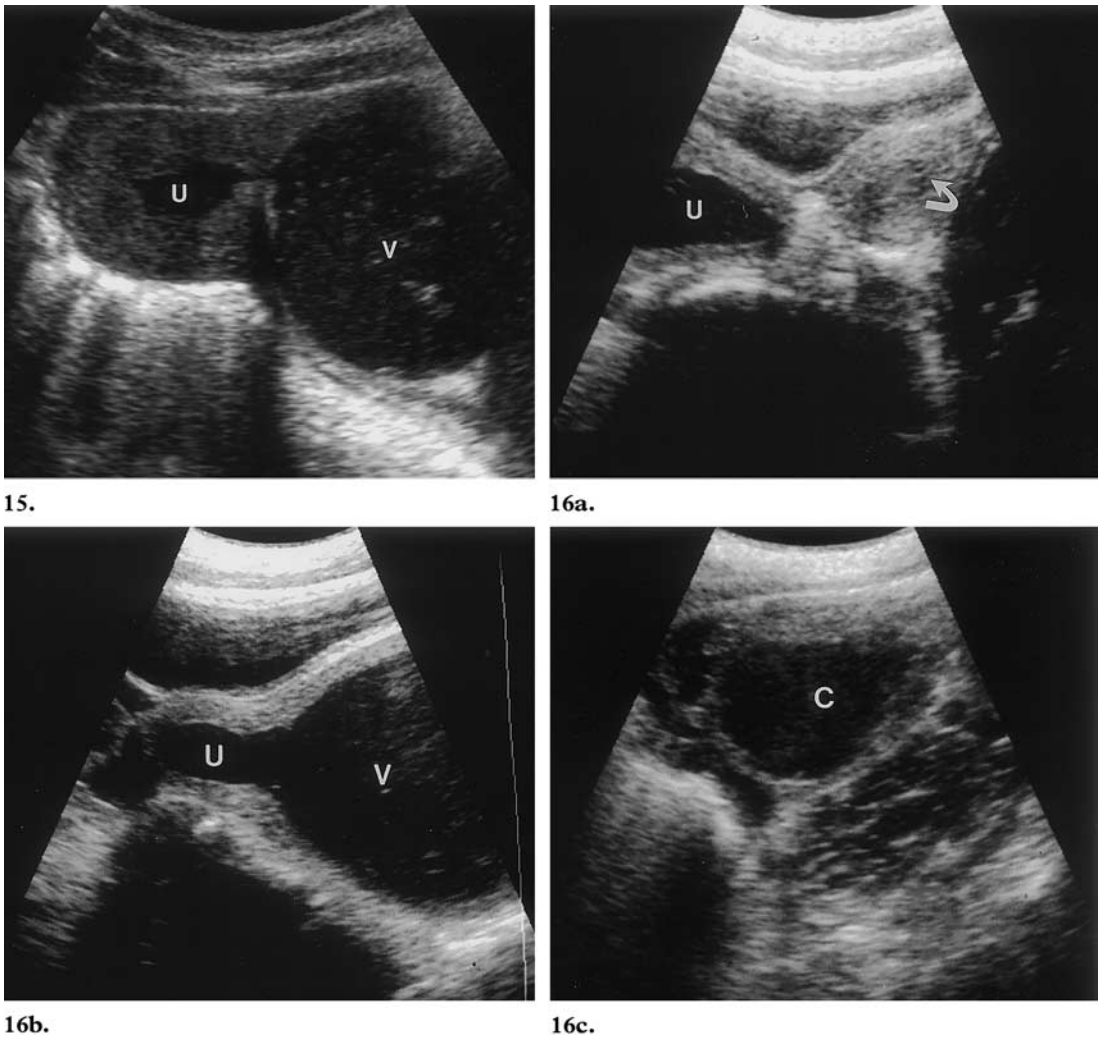

Figures 15, 16. **(15)** Hematometrocolpos due to an imperforate hymen in a 14-year-old girl with cyclic pelvic pain and primary amenorrhea. Longitudinal US scan shows a thin-walled, distended vagina (*V*) and the uterine cavity (*U*) with its thick myometrium. **(16)** Duplex uterus with an obstructed hemivagina in a 12-year-old girl. **(a)** Transverse US scan shows a normal left uterus (arrow) and a dilated right uterus (*U*). **(b)** Longitudinal US scan obtained along the obstructed side shows a distended vagina (*V*) and the dilated uterine cavity (*U*). The right kidney was absent. **(c)** Transverse US scan shows an endometrial cyst (*C*) adjacent to the ovary and the dilated fallopian tube.

due to cervical dysgenesis (26,31). Hematometrocolpos is cured by relieving the obstruction, whereas hematometra usually requires a hysterectomy. Approximately 45% of vaginal septa occur in the upper vagina, 40% in the middle vagina, and 15% in the lower vagina.

An obstructed hemivagina with a double uterus is almost always associated with ipsilateral renal agenesis (Fig 16). At clinical examination, cyclic abdominal pain (due to the obstruction) coexists with normal menses (through the unobstructed system).

When complete vaginal obstruction occurs, urgent attention is needed because of the risk of endometriosis and deterioration of reproductive capacity (Fig 16c).

Nonobstructive Müllerian Anomalies.—The main uterine configurations resulting from disorders of lateral fusion are septate, bicornuate, didelphys, and unicornuate. A longitudinal vaginal septum can be associated with uterine duplication defects (eg, uterus didelphys, uterus bicollis with a complete vaginal septum).

Diagnostic Value of US in Pediatric Patients with Pelvic Pain or Pelvic Masses

US is the initial imaging modality in children or adolescents with acute or subacute pelvic pain.

Ovarian Torsion

Ovarian torsion is more common in patients with predisposing lesions such as an ovarian cyst or an

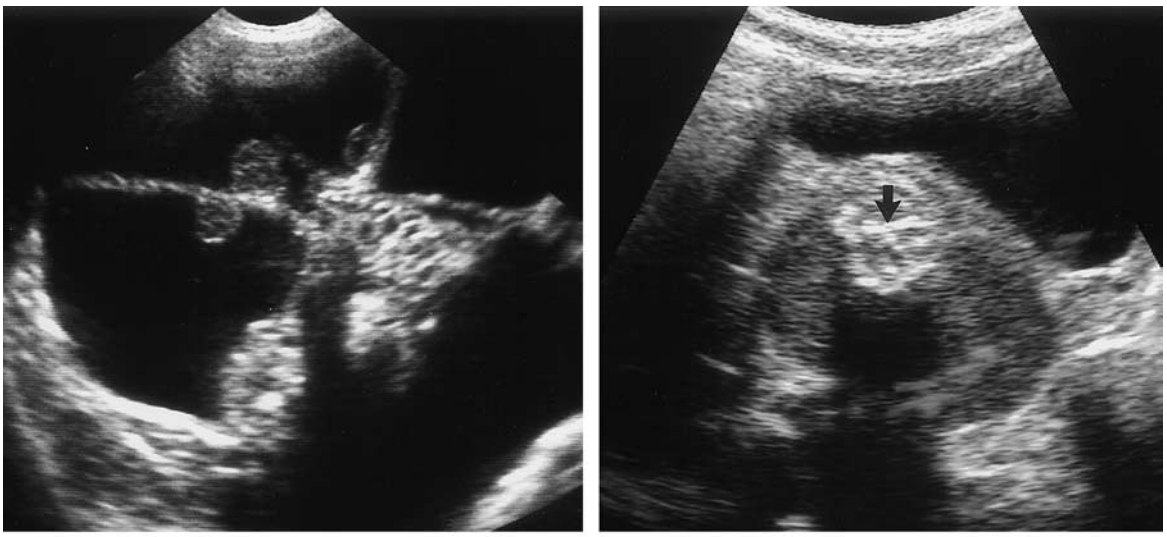

17. 18.

Figures 17, 18. **(17)** Immature ovarian teratoma in an 8-year-old girl. Longitudinal US scan shows a septated cystic mass with mural nodules. **(18)** Mature ovarian teratoma in a 2-year-old girl. Transverse US scan shows a solid retrovesical mass with a shadowing echogenic focus of calcium (arrow).

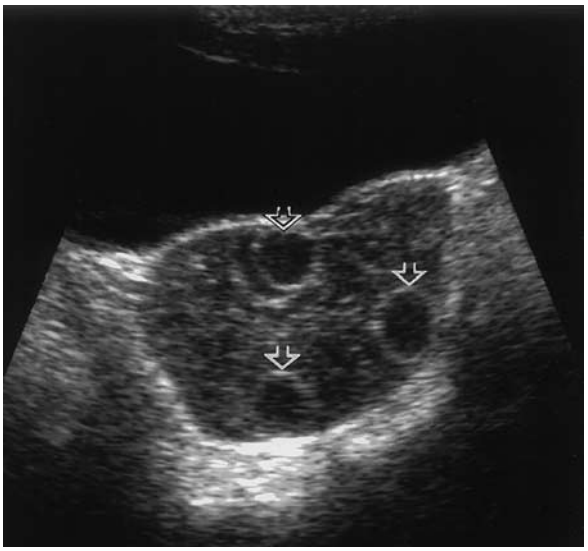

Figure 19. Torsion of a normal ovary in a 10-year-old girl with severe acute pelvic pain. Transverse US scan shows a markedly enlarged right ovary with peripheral follicles (arrows).

ovarian mass (teratoma) (32–34). In children, torsion of the normal ovary is also encountered because the fallopian tube is relatively long and the ovary is more mobile.

Ovarian Masses.—Ovarian masses in the pediatric age group consist of functional cysts in approximately 60% of cases and neoplasms in 40% of cases. Two-thirds of ovarian neoplasms are benign mature teratomas, one-third are malignant. At histologic analysis, ovarian malignancies in children are germ cell tumors in 60%–75% of cases, epithelial tumors in 10%–20%, and stromal tumors in approximately 10% (34).

Teratomas undergo torsion in 30% of cases and are bilateral in 10% of pediatric and adolescent cases. US shows mural nodules (55% of cases) (Fig 17) and echogenic foci with shadowing (44% of cases) (Fig 18), especially in postpubertal girls (35).

Indicators of malignancy at US are mostly the presence of peritoneal implants, ascites, lymphadenopathy, or hepatic metastases; the characteristics of the mass are less indicative.

Torsion of the Normal Ovary.—Torsion of the normal ovary is due to the excessive mobility of the ovary in the female child. The involved ovary appears markedly enlarged at US with multiple enlarged follicles at the periphery (Fig 19) (36); absence of flow at color Doppler US is not a reliable diagnostic criterion (37). Indeed, arterial flow (peripheral or even central) can be seen in surgically proved twisted ovaries. This finding has been demonstrated both in our clinical experience and in the literature (37) and may be explained by

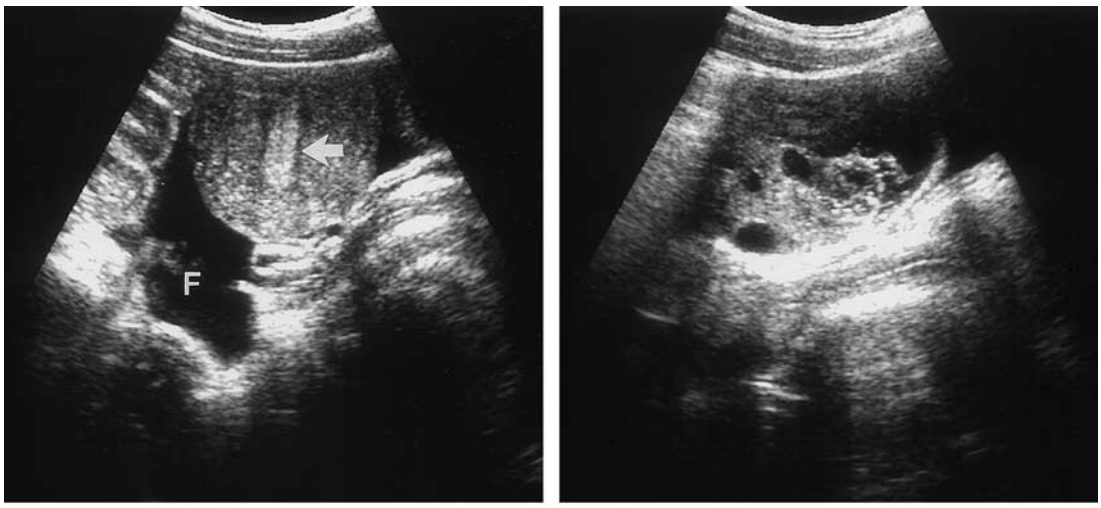

a. b.

Figure 20. Ruptured hemorrhagic ovarian cyst. **(a)** Longitudinal US scan of the uterus shows a prominent (midcycle) endometrium (arrow) and free peritoneal fluid (*F*). **(b)** Longitudinal US scan of the left ovary shows a complex adnexal mass adjacent to the ovarian parenchyma. Good through transmission is suggestive of the diagnosis initially.

the duality of ovarian arterial perfusion. Unfortunately, the ovary salvage rate in cases of torsion is low due to delays in diagnosis and intervention.

Hemorrhagic Ovarian Cyst

Severe acute pelvic pain contemporary with the midcycle is clinically suggestive of hemorrhage within a functional ovarian cyst (corpus luteum cyst). US shows a complex adnexal mass with increased through transmission, reflecting its cystic nature; free fluid can often be observed (Fig 20) (38). At follow-up US, the cyst again becomes predominantly anechoic.

Pelvic Inflammatory Disease and Tubo-ovarian Abscess

Pelvic inflammatory disease in sexually active adolescents is recognized on the basis of clinical criteria (pelvic pain, fever, cervical motion, adnexal tenderness) and laboratory criteria (*Chlamydia trachomatis* in 45% of cases). US is useful only to detect complications such as hydrosalpinx or tubo-ovarian abscess.

Ectopic Pregnancy

Ectopic pregnancy has the lowest rate among adolescents, but this age group has the highest reported death rate. As in adults, endovaginal US correlated with quantitative assessment of beta human chorionic gonadotropin is the essential diagnostic test.

Contribution of US in Patients with Ambiguous Genitalia

In the male fetus, sexual differentiation is hormonally mediated by means of production of antimüllerian hormone and testosterone by the fetal testes (Fig 21). Conversely, in the female fetus, sexual differentiation is basically an autonomous process.

US is very effective in demonstrating the presence or absence of a uterus in newborns with ambiguous genitalia (39). Most cases of ambiguous genitalia consist of female pseudohermaphroditism due to congenital adrenal hyperplasia; in these cases, US shows a normal uterus and ovaries (Fig 22). Increased size of the adrenal glands has been reported in newborns and infants with congenital adrenal hyperplasia (40).

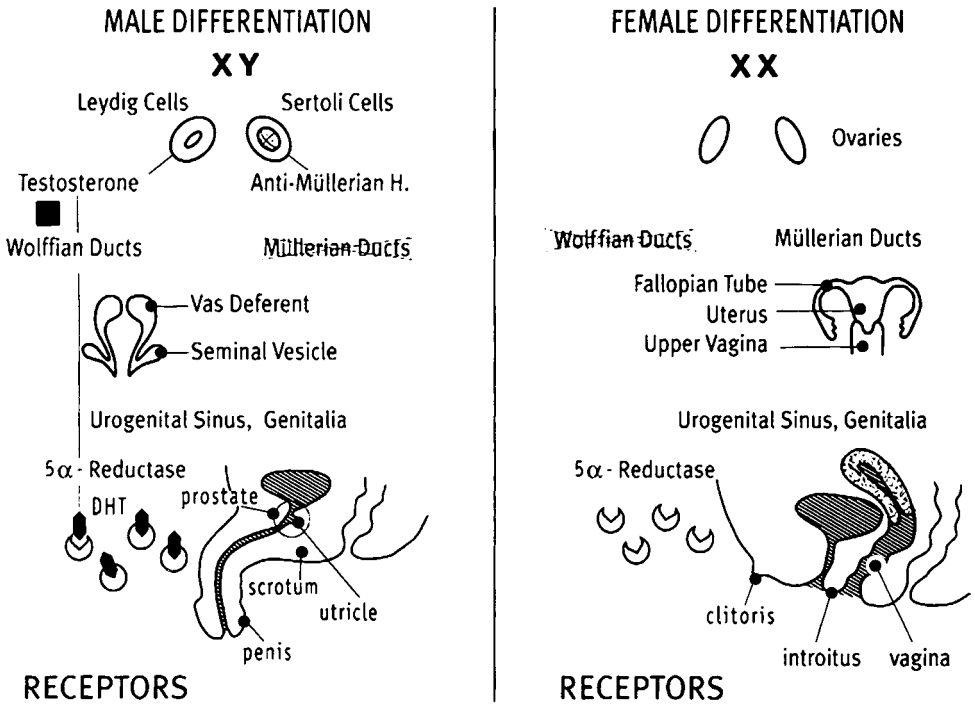

Figure 21. Sexual differentiation in the fetus. Left: Diagram shows that adequate male differentiation needs the activity of two fetal testicular hormones, antimüllerian hormone and testosterone. The former contributes to regression of the müllerian ducts; the latter contributes to masculinization of the wolffian ducts and the urogenital sinus after reduction of dihydrotestosterone (*DHT*). *H* = hormone. Right: Diagram shows that the process is autonomous in the female. The müllerian ducts persist in the absence of antimüllerian hormone, and the wolffian ducts regress in the absence of testosterone.

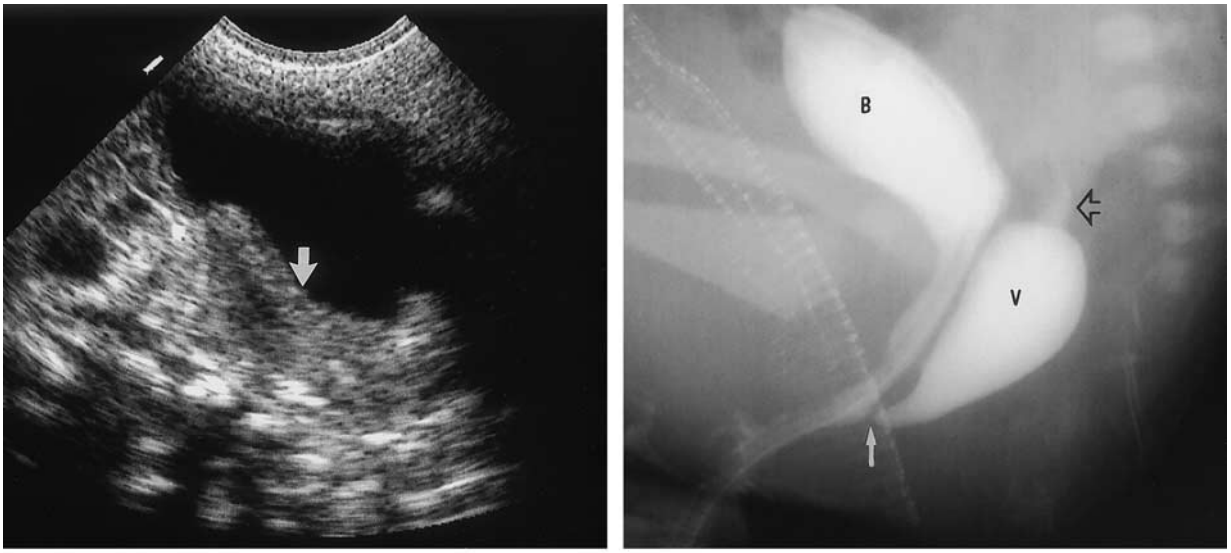

a. **b.**

Figure 22. Ambiguous genitalia in a newborn with congenital adrenal hyperplasia. **(a)** Longitudinal US scan shows a normal uterus (arrow). **(b)** Lateral image from genitography shows urethrovaginal confluence (solid arrow) and partial opacification of the uterine cavity (open arrow). *B* = bladder, *V* = vagina.

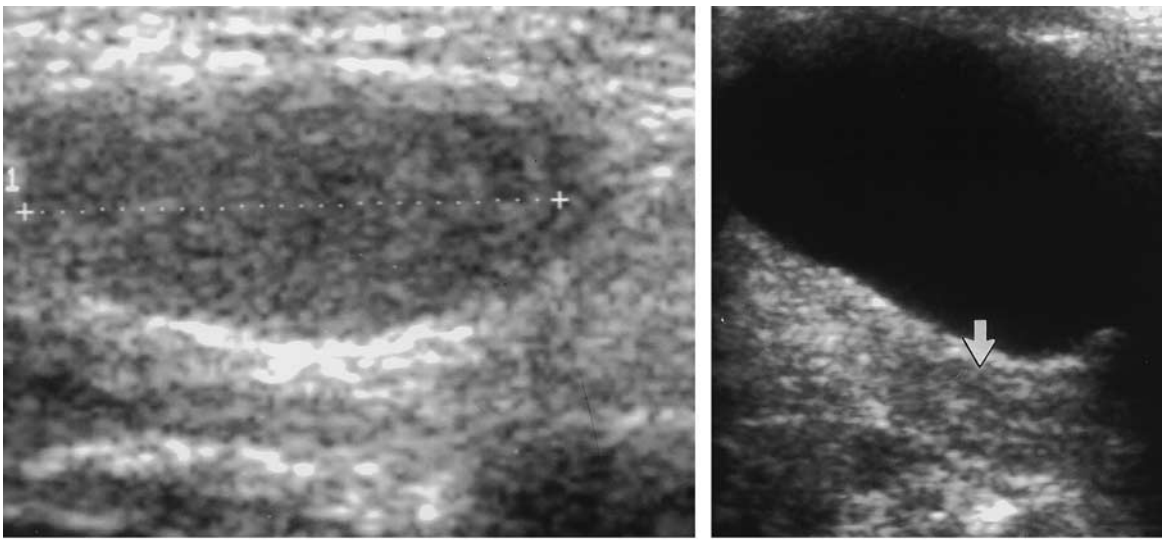

a. b.

Figure 23. Ambiguous genitalia in a newborn with true hermaphroditism. **(a)** Longitudinal US scan of the inguinal region shows a testicular echostructure (between cursors). **(b)** Longitudinal US scan of the pelvis shows a uterus (arrow).

In the rare cases of male pseudohermaphroditism or true hermaphroditism, high-frequency transducers can also demonstrate testicular parenchyma (Fig 23).

Conclusions

Because of its innocuousness, simplicity, and reliability, US is very useful in imaging genital organs in infants and children. Its value in assessing the anatomy and the hormonal status of children with sexual precocity or delay must be emphasized. As an initial imaging modality, US is also valuable in cases of pelvic pain or pelvic masses in the pediatric age group. CT remains useful for tumor staging and follow-up. Magnetic resonance imaging provides precise demonstration of anatomic features in multiple planes in cases of complex anomalies when US findings are incomplete or inconclusive (41).

Acknowledgment: The authors thank Ginette Bleau for her dedication and great skill in preparing and editing the manuscript.

References

1. Bridges NA, Cooke A, Healy MJ, Hindmarsh PC, Brook CG. Growth of the uterus. Arch Dis Child 1996; 75:330–331.
2. Nussbaum AR, Sanders RC, Jones MD. Neonatal uterine morphology as seen on real-time US. Radiology 1986; 160:641–643.
3. Hata K, Nishigaki A, Makihara K, Takamiya O, Hata T, Kitao M. Ultrasonic evaluation of the normal uterus in the neonate. J Perinat Med 1989; 17:313–317.
4. Haber HP, Mayer EI. Ultrasound evaluation of uterine and ovarian size from birth to puberty. Pediatr Radiol 1994; 24:11–13.
5. Holm K, Laursen EM, Brocks V, Muller J. Pubertal maturation of the internal genitalia: an ultrasound evaluation of 166 healthy girls. Ultrasound Obstet Gynecol 1995; 6:175–181.
6. Buzi F, Pilotta A, Dordoni D, Lombardi A, Zaglio S, Adlard P. Pelvic ultrasonography in normal girls and in girls with pubertal precocity. Acta Paediatr 1998; 87:1138–1145.
7. Griffin IJ, Cole TJ, Duncan KA, Hollman AS, Donaldson MD. Pelvic ultrasound measurements in normal girls. Acta Paediatr 1995; 84:536–543.
8. Orbak Z, Sagsoz N, Alp H, Tan H, Yildirim H, Kaya D. Pelvic ultrasound measurements in normal girls: relation to puberty and sex hormone concentration. J Pediatr Endocrinol Metab 1998; 11:525–530.
9. Cohen HL, Shapiro MA, Mandel FS, Shapiro ML. Normal ovaries in neonates and infants: a sonographic study of 77 patients 1 day to 24 months old. AJR Am J Roentgenol 1993; 160: 583–586.
10. Orsini LF, Salardi S, Pilu G, Bovicelli L, Cacciari E. Pelvic organs in premenarcheal girls: real-time ultrasonography. Radiology 1984; 153:113–116.
11. Cohen HL, Eisenberg P, Mandel F, Haller JO. Ovarian cysts are common in premenarchal girls: a sonographic study of 101 children 2–12 years old. AJR Am J Roentgenol 1992; 159:89–91.
12. Haber HP, Wollmann HA, Ranke MB. Pelvic ultrasonography: early differentiation between isolated premature thelarche and central precocious puberty. Eur J Pediatr 1995; 154:182–186.
13. Caspi B, Zalel Y, Katz Z, Appelman Z, Insler V. The role of sonography in the detection of vaginal foreign bodies in young girls: the bladder indentation sign. Pediatr Radiol 1995; 25(suppl 1):S60–S61.

14. Martelli H, Oberlin O, Rey A, et al. Conservative treatment for girls with nonmetastatic rhabdomyosarcoma of the genital tract: a report from the Study Committee of the International Society of Pediatric Oncology. J Clin Oncol 1999; 17:2117–2122.
15. Andrassy RJ, Wiener ES, Raney RB, et al. Progress in the surgical management of vaginal rhabdomyosarcoma: a 25-year review from the Intergroup Rhabdomyosarcoma Study Group. J Pediatr Surg 1999; 34:731–734.
16. Ambrosino MM, Hernanz-Schulman M, Genieser NB, Sklar CA, Fefferman NR, David R. Monitoring of girls undergoing medical therapy for isosexual precocious puberty. J Ultrasound Med 1994; 13:501–508.
17. Jensen AM, Brocks V, Holm K, Laursen EM, Muller J. Central precocious puberty in girls: internal genitalia before, during, and after treatment with long-acting gonadotropin-releasing hormone analogues. J Pediatr 1998; 132:105–108.
18. Low LC, Wang C, Leung A, Leong LY. Undetectable levels of serum FSH immunoactivity and bioactivity in girls with sexual precocity due to ovarian cysts. Acta Paediatr 1994; 83:623–626.
19. Rodriguez-Macias KA, Thibaud E, Houang M, Duflos C, Beldjord C, Rappaport R. Follow up of precocious pseudopuberty associated with isolated ovarian follicular cysts. Arch Dis Child 1999; 81:53–56.
20. Fakhry J, Khoury A, Kotval PS, Noto RA. Sonography of autonomous follicular ovarian cysts in precocious pseudopuberty. J Ultrasound Med 1988; 7:597–603.
21. Lee HJ, Woo SK, Kim JS, Suh SJ. "Daughter cyst" sign: a sonographic finding of ovarian cyst in neonates, infants, and young children. AJR Am J Roentgenol 2000; 174:1013–1015.
22. Haber HP, Ranke MB. Pelvic ultrasonography in Turner syndrome: standards for uterine and ovarian volume. J Ultrasound Med 1999; 18:271–276.
23. Shawker TH, Garra BS, Loriaux DL, Cutler GB Jr, Ross JL. Ultrasonography of Turner's syndrome. J Ultrasound Med 1986; 5:125–129.
24. Mazzanti L, Nizzoli G, Tassinari D, et al. Spontaneous growth and pubertal development in Turner's syndrome with different karyotypes. Acta Paediatr 1994; 83:299–304.
25. Matarazzo P, Lala R, Artesani L, Franceshini PG, De Sanctis C. Sonographic appearance of ovaries and gonadotropin secretions as prognostic tools of spontaneous puberty in girls with Turner's syndrome. J Pediatr Endocrinol Metab 1995; 8:267–274.
26. Rock JA. Anomalous development of the vagina. Semin Reprod Endocrinol 1986; 4:13–31.
27. Rosenberg HK, Sherman NH, Tarry WF, Duckett JW, Snyder HM. Mayer-Rokitansky-Kuster-Hauser syndrome: US aid to diagnosis. Radiology 1986; 161:815–819.
28. Carranza-Lira S, Forbin K, Martinez-Chequer JC. Rokitansky syndrome and MURCS association: clinical features and basis for diagnosis. Int J Fertil Womens Med 1999; 44:250–255.
29. Blask AR, Sanders RC, Gearhart JP. Obstructed uterovaginal anomalies: demonstration with sonography. I. Neonates and infants. Radiology 1991; 179:79–83.
30. Banerjee AK, Clarke O, MacDonald LM. Sonographic detection of neonatal hydrometrocolpos. Br J Radiol 1992; 65:268–271.
31. Blask AR, Sanders RC, Rock JA. Obstructed uterovaginal anomalies: demonstration with sonography. II. Teenagers. Radiology 1991; 179:84–88.
32. Surratt JT, Siegel MJ. Imaging of pediatric ovarian masses. RadioGraphics 1991; 11:533–548.
33. Brown MF, Hebra A, McGeehin K, Ross AJ 3rd. Ovarian masses in children: a review of 91 cases of malignant and benign masses. J Pediatr Surg 1993; 28:930–933.
34. Gribbon M, Ein SH, Mancer K. Pediatric malignant ovarian tumors: a 43-year review. J Pediatr Surg 1992; 27:480–484.
35. Sisler CL, Siegel MJ. Ovarian teratomas: a comparison of the sonographic appearance in prepubertal and postpubertal girls. AJR Am J Roentgenol 1990; 154:139–141.
36. Graif M, Itzchak Y. Sonographic evaluation of ovarian torsion in childhood and adolescence. AJR Am J Roentgenol 1988; 150:647–649.
37. Stark JE, Siegel MJ. Ovarian torsion in prepubertal and pubertal girls: sonographic findings. AJR Am J Roentgenol 1994; 163:1479–1482.
38. Baltarowich OH, Kurtz AB, Pasto ME, Rifkin MD, Needleman L, Goldberg BB. The spectrum of sonographic findings in hemorrhagic ovarian cysts. AJR Am J Roentgenol 1987; 148:901–905.
39. Kutteh WH, Santos-Ramos R, Ermel LD. Accuracy of ultrasonic detection of the uterus in normal newborn infants: implications for infants with ambiguous genitalia. Ultrasound Obstet Gynecol 1995; 5:109–113.
40. Al-Alwan I, Navarro O, Daneman D, Daneman A. Clinical utility of adrenal ultrasonography in the diagnosis of congenital adrenal hyperplasia. J Pediatr 1999; 135:71–75.
41. Lang IM, Babyn P, Oliver GD. MR imaging of paediatric uterovaginal anomalies. Pediatr Radiol 1999; 29:163–170.

This article meets the criteria for 1.0 credit hour in category 1 of the AMA Physician's Recognition Award. To obtain credit, see www.rsna.org/education/rg_cme.html.